6 September 2024
jakub.maly@cern.ch

Computing conversion coefficients between different quantities used for radiation measurements at the CERN accelerator complex

Jakub Malý
Supervisors: Auriane Canesse, Daniel Prelipcean
SY-STI-BMI, CERN, Geneva, Switzerland

Keywords: Radiation, Conversion Coefficients, R2E, MCWG, FLUKA

Summary

This work details my summer student project, for which I created a framework for computing conversion coefficients between several different radiation quantities used by the R2E project. I then used data from 2022 (LHC run 3) for the LHC Interaction Point 1 (IP1; ATLAS detector and the tunnels around it) to compute conversion coefficients at the locations of radiation measurement devices and compared simulation data to measurements.

Contents

1 Introduction

Large amounts of high-energy particle interactions lead to high radiation levels. At the CERN accelerator complex, there are three main sources of prompt (primary) radiation: direct collisions (such as the proton-proton collisions at the Large Hadron Collider); beam-machine interactions (when the beam collides with collimators or beam intercepting devices); and beam-gas interactions (where the beam interacts with residual gas in the beam pipe).

The Monitoring and Calculation Working Group (MCWG)—part of the larger Radiation to Electronics (R2E) activity[1]—characterises prompt radiation at the CERN accelerator complex through measurements and simulations for the purposes of machine protection. Information about the radiation environment is then used for a multitude of purposes, which include guiding future design for materials and electronics as well as determining when current equipment needs to be replaced. Therefore, accurately understanding the radiation environment is crucial for the reliable operation of the CERN accelerator complex.

As my summer student project, I created a framework for computing conversion coefficients between several different radiation quantities used in the R2E activity. I then used data from 2022 (LHC run 3) for the LHC Interaction Point 1 (IP1; ATLAS detector and the tunnels around it) to compute conversion coefficients at the locations of radiation measurement devices and compared simulation data to measurements. This work expands on a previous study presented during the 44th MCWG meeting.[2]

2 Radiation at the LHC

Radiation at the CERN accelerator complex can be divided into two parts: cumulative damage experienced by all materials, and single-event effects that are mostly relevant for electronics. This section details what quantities are used to describe radiation, the specifics of how radiation particles cause damage, and the different types of radiation measurement devices used.

Note that this work (and the work of MCWG at large) only considers prompt radiation—radiation that is caused by the beam interacting with another beam or the surrounding machinery. Therefore, all secondary radiation (such as radiation from activated materials) will not be discussed, as it is within the mandate of the Radiation Protection (RP) group at CERN.

2.1 Cumulative damage

The main quantity used for describing cumulative damage is the total ionising dose (TID). It quantifies the amount of energy deposited in a material, and the corresponding SI unit is a gray: Gy = J/kg. Data in this work is normalised per inverse femtobarn of delivered beam luminosity, so the unit is also normalised as $\mathrm{Gy/fb^{-1}}$. Note that while deposited energy does not cause damage directly, we expect the cumulative material damage to scale with the TID received. There are several devices we use for measuring TID: beam loss monitors (BLMs, Section 4.2.1); radio-photo-luminescent dosimeters (RPLs); distributed optical fibres for radiation sensing (DOFRS); and radiation monitors (RadMons, Section 4.2.2). However, this report focuses on BLM and RadMon data due to their comparatively high fidelity.

The second quantity used for cumulative damage is the silicon 1 MeV neutron equivalent fluence (time integrated particle flux), expressed in neutrons/cm^2/fb^{-1}. As the name implies, this quantity is relevant for silicon, where neutrons at the energy scale of 1 MeV can displace atoms from the silicon lattice, creating what is known as Frenkel defects. These defects degrade the material's electrical properties and therefore the performance of semiconductors. We can measure this quantity using radiation monitors (RadMons), but we currently have little data, so this quantity will be obtained from simulations.

2.2 Single-event effects

The main source of non-destructive single-event effects (such as bit flips) are thermal neutrons. The corresponding radiation quantity is the thermal neutron equivalent fluence (THN Eq.), with units of neutrons/cm^2/fb^{-1}. They are called thermal because the neutrons have kinetic energy similar to the thermal (kinetic) energy of matter around them, which leads to a large interaction cross-section (probability) of the neutron with matter.

On the other hand, destructive single-event effects are mostly caused by high-energy hadrons—particles made up of quarks. These include the beam protons themselves, as well as neutrons, heavy ions, pions, kaons, and other exotic hadronic states. The destructive power of high energy hadrons comes from the fact that they have a large interaction cross-section with nuclei which they can either displace or destroy depending on the amount of energy transferred. The corresponding R2E quantity is the high energy hadron equivalent fluence (HEH Eq.), with units of hadrons/cm^2/fb^{-1}.

Both thermal neutrons and high energy hadrons are measured using radiation monitors (RadMons), detailed in Section 4.2.2. These are either fixed-location devices; deployed radiation monitors (connected to a fixed RadMon via a cable); or battery-powered (the so-called BatMon).

3 Why we need conversion coefficients

Unlike TID, for which we have high fidelity data due to a large amount of measurement devices, we do not have much data for thermal neutron fluence nor high energy hadron fluence, which we can only measure using radiation monitors. As illustrated in Figure 1, we have data from only six RadMons around the ATLAS detector (and not all of them have both THN Eq. and HEH Eq. data), whereas there are 134 BLMs.

We currently use an order-of-magnitude estimate for converting from TID to other radiation quantities—1 Gy is equal to 10^9 hadrons or 10^{10} neutrons.[3] However, when we plot the ratios of particle fluences to TID

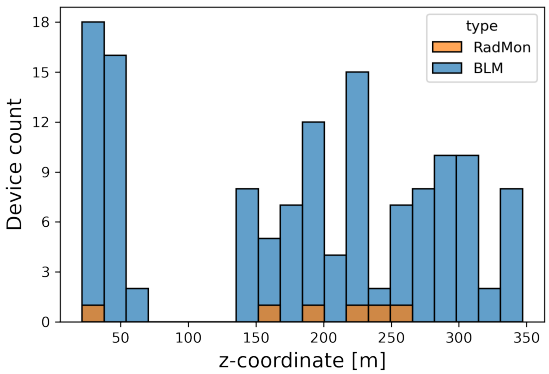

Figure 1: LHC IP1: Number of measurement devices around the ATLAS detector ($z = 0$ m). Devices from left and right side are merged; z-coordinate corresponds to beam direction.

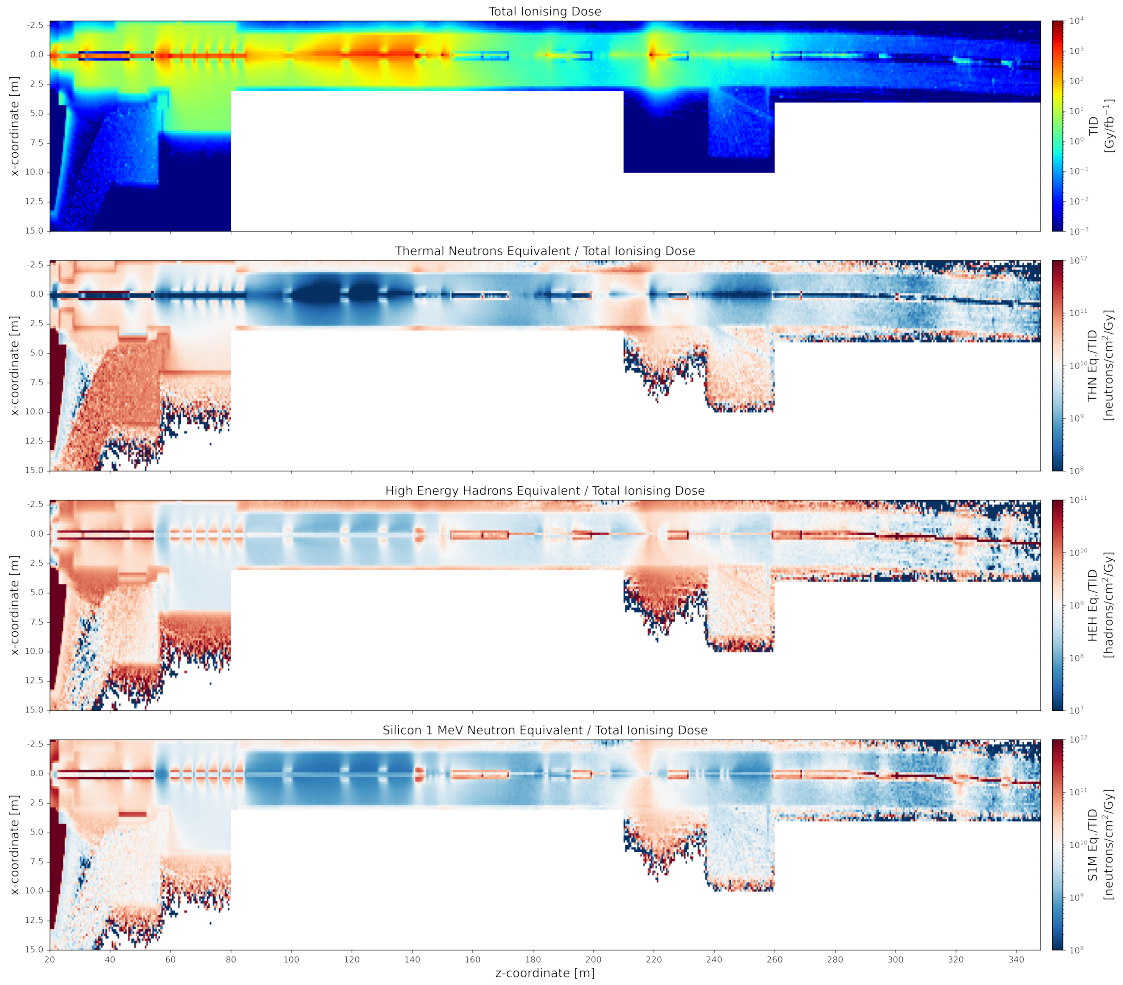

Figure 2: LHC IP1: Total ionising dose (TID) simulation data (mean value around beam height $y = 0 \pm 0.2$ m). Ratio colour maps are centered at order-of-magnitude estimates currently used. The coefficient ratio data was truncated at two orders of magnitude above and below the current order-of-magnitude estimates to remove outliers and improve clarity.

in Figure 2, we can see that the radiation environment has a range of about four orders of magnitude. More specifically, radiation seems to be higher in the shielded alcoves, and lower in the long straight section (LSS) of the tunnel.

Simulations have their own set of features and issues—they require extensive computational resources (e.g. the simulation data used in this work was obtained with 10^5 CPU hours, equivalent to 11.4 CPU years), and they only reflect one static operational configuration of the machine. Therefore, we want to combine conversion coefficients computed from simulations with TID measurement data to achieve results that are as close to the real radiation environment as we can get.

4 Conversion coefficient framework

Obtaining the conversion coefficients can be described as a four step process:

1. extract location of interest;
2. extract data from simulations at these locations;
3. compute coefficients from simulation data;
4. validate results via comparison to measurements.

In practice, this first requires parsing, formatting, and merging data from several sources. This includes parsing simulation binaries (Section 4.1); matching device names from the layout database to measurements taken from the MCWG dashboard; and then saving the data into a single standardised format.

Decoupling dataset pre-processing from the actual coefficient computation allows us to maintain a high level of modularity. All datasets are first pre-processed and saved in a CSV format, and then the conversion coefficients are calculated and plotted.

The framework is written in Python. Not only is this a popular language, but this allows us to use other Python tooling—from interfacing with CERN's `NXCALS` database, which provides reliable and efficient access to the large volume of data produced at CERN, to using `PyROOT` for data analysis. Since the combined simulation datasets are over a gigabyte in size, I decided to use the `polars` library for the framework back-end, since it provides light-weight dataframes with support for fast, multi-threaded, and lazy operations.

4.1 Simulation data

The simulations were made using `FLUKA`[4;5;6]—a Monte Carlo simulation package developed at CERN for simulating interactions and transport of particles and nuclei in matter.

Data used in this project was obtained from `FLUKA` version 4.3.3, simulating proton-proton collisions through a simplified geometry of the LHC IP1 tunnel with the collision point at $x = y = z = 0$. The parameters were consistent with the measurement period of 2022. Unlike the 2018 simulations (LHC run 2), which were focused on generic radiation environment studies, the 2022 (LCH run 3) simulations had larger bin sizes—$20 \times 20 \times 50$ cm, compared to $10 \times 10 \times 10$ cm for 2018 bins—meaning the data has lower resolution. The 2018 data could also be analysed (and is included in the GitLab repository),[7] but this report focuses on the 2022 measurements and simulations only.

4.2 Measurement data

The measurement data was obtained from MCWG's Grafana dashboard[8;9] and covers the 2022 calendar year. All measured radiation quantities were normalised by the integrated luminosity delivered to ATLAS in 2022, equalling $\mathcal{L}_{\text{int}} = 41.1\ \text{fb}^{-1}$. Since some RadMons were not operational throughout the whole year, their normalisation luminosity was determined via the integrated luminosity delivered during their operation period.

The position data was obtained from CERN's layout database. Therefore, it is assumed that the positions of the devices have not changed in the last two years. Measurement devices that did not have positional data were discarded—this included about two thirds of all radiation monitors (RadMons).

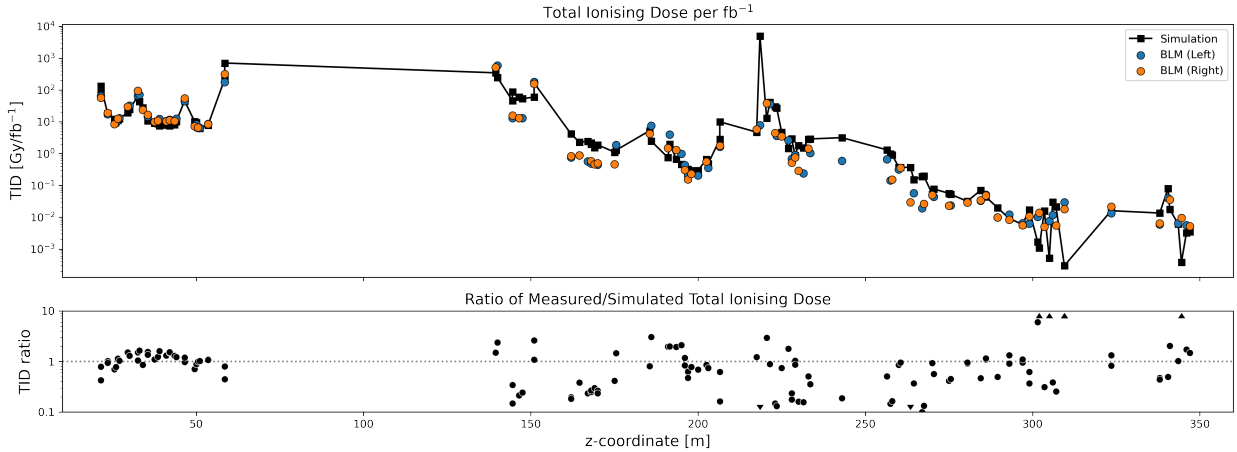

Figure 3: LHC IP1: Comparison between measured and simulated total ionising dose (TID). Top: Beam loss monitor (BLM) measurements of TID and simulated TID at BLM coordinates (z-coordinate shown as absolute value, since simulation is symmetric).
Bottom: Ratio of measurement-to-simulation; arrows point to outliers outside the y-range.

4.2.1 Beam Loss Monitors (BLM)

Beam loss monitors' primary function is measuring TID rates as fast as possible for machine protection. The ionising dose delivered is measured via ionisation chambers, and detection of abnormal dose levels triggers a beam dump to avoid quenches of superconducting magnets. R2E has developed methods to extract total ionising dose data from beam loss monitors, but there are limitations to this methodology. [9;10]

4.2.2 Radiation Monitors (RadMon)

The radiation monitors, on the other hand, were purpose-built for measuring several R2E quantities: total ionising dose, high energy hadron fluence equivalent, and thermal neutron fluence equivalent. [11] However, they cannot be deployed in areas reaching above a couple hundred grays per year due to them not being very radiation-hard. From a more practical perspective, many RadMons did not have enough data to compute conversion coefficients (0 or 1 of the 3 quantities measured), or had un-physical TID evolutions, and were discarded.

5 LHC IP1: Case study results

As we can see in Figure 3, the agreement between measured and simulated TID is mostly within one order of magnitude. While this may look like a large difference, it is smaller than the two orders of magnitude differences we saw in Figure 2 for estimating particle fluences from TID. Moreover, most of the uncertainty comes from data points further from the collisions at $z = 0$. This is a compounding of a smaller number of proton primaries reaching this far, and simulation artefacts where a particle below the energy threshold (usually a few keV) immediately dumps all its energy in one place and is deleted.

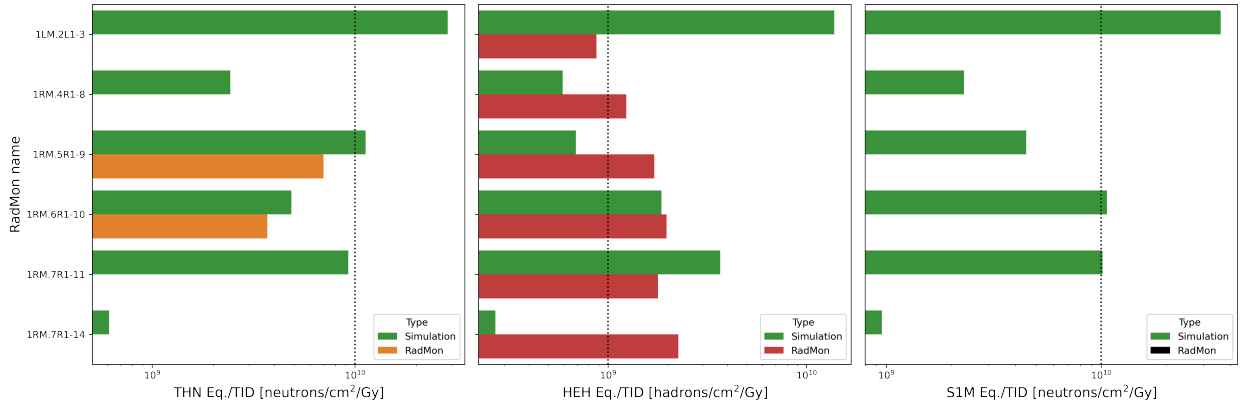

Figure 4: LHC IP1: Simulated radiation coefficients at RadMon locations (green) and measurement ratios (orange, red). Dashed lines show order-of-magnitude estimates currently used.

We can also compare the simulated and measured coefficients with the current order-of-magnitude estimates (Figure 4). Here, we see that while some RadMon data matches very well with simulations—and matches better than the current estimates shown as dashed lines—the first and last RadMon have a very large difference in high energy hadron fluence and lack thermal neutron fluence measurements altogether. While this is not good, we can use large differences like these to identify measurement devices which may need further manual scrutiny.

6 Conclusion

The results of this work include a Python framework for cleaning and combining datasets; computing conversion coefficients for simulations; comparing simulations with measurements; and plotting utilities to display the data.[7] The LHC IP1 results include a set of fully documented pre-processed datasets for both simulation and measurement data, as well as a dataset of conversion coefficients at BLM and RadMon locations, which are to be added to the MCWG dashboard. Unfortunately, I did not have time to include simulation errors into the framework, but it should be possible to add these with minimal tweaks to the dataset parsing code.

The framework can be used to compute conversion coefficients between any two R2E quantities from `FLUKA` simulation data. As such, it can be used for any part of the CERN accelerator complex in the future. Furthermore, the separation between pre-processing and coefficient calculation allows the code to be highly maintainable and re-usable.

References

[1] Radiation to Electronics (R2E) project at CERN. *CERN*. URL https://r2e.web.cern.ch.

[2] D. Prelipcean. 44th MCWG meeting, Conversion coefficients between different quantities measuring radiation levels at the LHC. URL https://indico.cern.ch/event/978953/.

[3] K. Bilko M. Sabaté Gilarte C. Bahamonde Castro A. Lechner O. Stein A. Tsinganis F. Cerutti Y. Kadi G. Lerner, R. García Alía. HL-LHC Radiation level specification document, 2302154 v.1.0—LHC-N-ES-0001 v.1.0. Technical report, CERN, 2020.

[4] The official CERN FLUKA website. *CERN*. URL https://fluka.cern.

[5] C. Ahdida, D. Bozzato, D. Calzolari, F. Cerutti, N. Charitonidis, A. Cimmino, A. Coronetti, G. L. D'Alessandro, A. Donadon Servelle, L. S. Esposito, R. Froeschl, R. García Alía, A. Gerbershagen, S. Gilardoni, D. Horváth, G. Hugo, A. Infantino, V. Kouskoura, A. Lechner, B. Lefebvre, G. Lerner, M. Magistris, A. Manousos, G. Moryc, F. Ogallar Ruiz, F. Pozzi, D. Prelipcean, S. Roesler, R. Rossi, M. Sabaté Gilarte, F. Salvat Pujol, P. Schoofs, V. Stránský, C. Theis, A. Tsinganis, R. Versaci, V. Vlachoudis, A. Waets, and M. Widorski. New Capabilities of the FLUKA Multi-Purpose Code. *Frontiers in Physics*, 9, 01 2022. doi: 10.3389/fphy.2021.788253.

[6] G. Battistoni, T. Boehlen, F. Cerutti, P.W. Chin, L.S. Esposito, A. Fassò, A. Ferrari, A. Lechner, A. Empl, A. Mairani, A. Mereghetti, P. Garcia Ortega, J. Ranft, S. Roesler, P.R. Sala, V. Vlachoudis, and G. Smirnov. Overview of the FLUKA code. *Annals Nucl. Energy*, 82: 10–18, 2015. doi: 10.1016/j.anucene.2014.11.007.

[7] J. Malý. Summer Student Project—Framework for computing conversion coefficients between different radiation quantities used at the CERN accelerator complex. *GitLab*, 2024. URL https://gitlab.cern.ch/mcwg/lhc/Fluka_and_BLMs_IR1_and_IR5_analyses/ir1-ratio-analysis.

[8] Radiation to Electronics (R2E) Monitoring Dashboard. *CERN*. URL https://r2e-monitoring.web.cern.ch.

[9] K. Biłko, R. García Alía, and J.B. Potoine. Automated Analysis of the Prompt Radiation Levels in the CERN Accelerator Complex. In *Proc. IPAC'22*, number 13 in International Particle Accelerator Conference, pages 736–739. JACoW Publishing, Geneva, Switzerland, 07 2022. ISBN 978-3-95450-227-1. doi: 10.18429/JACoW-IPAC2022-MOPOMS043. URL https://jacow.org/ipac2022/papers/mopoms043.pdf.

[10] B. Dehning, E. Effinger, J. Emery, G. Ferioli, G. Guaglio, E. B. Holzer, D. Kramer, L. Ponce, V. Prieto, M. Stockner, and C. Zamantzas. The LHC beam loss measurement system. In *2007 IEEE Particle Accelerator Conference (PAC)*, pages 4192–4194, 2007. doi: 10.1109/PAC.2007.4439980.

[11] G. Spiezia, P. Peronnard, A. Masi, M. Brugger, M. Brucoli, S. Danzeca, R. Garcia Alia, R. Losito, J. Mekki, P. Oser, R. Gaillard, and L. Dusseau. A New RadMon Version for the LHC and its Injection Lines. *IEEE Transactions on Nuclear Science*, 61(6):3424–3431, 2014. doi: 10.1109/TNS.2014.2365046.